A Simple, Vertically Resolved Model of Tropical Disturbances With a Humidity Closure

Željka Fuchs* and David J. Raymond

December 15, 2006

Physics Department and Geophysical Research Center, New Mexico Institute of Mining and Technology, Socorro, New Mexico, 87801 USA

Abstract

A vertically resolved linear model for large-scale motions in an equatorial non-rotating atmosphere is presented. Precipitation is forced by tropospheric precipitable water, cloud-radiation interactions (CRI), and wind-induced surface heat exchange (WISHE). The dynamics of the model are based on the assumption that the vertical heating profile has the shape of the first baroclinic mode. The vertical profiles of vertical velocity, temperature perturbation, etc. are calculated using an upward radiation boundary condition.

The modeled modes are of three types: fast gravity waves that resemble adiabatic modes with the vertical wavelength twice the depth of the troposphere; convectively coupled gravity modes that are damped and move with a phase speed of ≈ 17 m s^{-1}; and the unstable moisture mode.

The value of the model is that under a single dynamical assumption it yields the observed phase speed for the convectively coupled gravity waves that map to Kelvin waves in the equatorial beta plane case while still producing the unstable moisture mode. However, the model lacks the precipitation physics needed to produce the observed destabilization of the gravity mode.

1 Introduction

Many hypotheses about the interaction of deep convection and large-scale flows in the tropics have been tested first in simplified linear models. Such models are good test beds because convective interactions are more transparent than in complex weather prediction

* Corresponding author Email: tzeljka@nmt.edu

models. In addition, tropical, convectively coupled wave modes provide an excellent test of linearized models (Wheeler and Kiladis, 1999). To provide context for the work in this paper, we first present a discussion of existing conceptual models of the interaction between convection and the large scale.

1.1 Ekman pumping

Charney and Eliassen (1964) and Charney (1971) hypothesized that Ekman pumping caused boundary layer air to rise to the level of free convection, thus forcing deep convection in tropical storms and in the intertropical convergence zone (ITCZ). This idea has been very robust, being expressed in the Kelvin-Rossby wave theory of Wang and Rui (1990; see also Moskowitz and Bretherton, 2000) and in models such as those of Lindzen and Nigam (1987) and Battisti et al. (1999). This theory has some skill in predicting at least the time-averaged position of the ITCZ (Tomas et al. 1999; McGauley et al. 2004). However, Raymond et al., (2006) present evidence that Ekman pumping is a poor guide to the day-to-day location of deep convection in the tropics.

1.2 Wave-CISK

Hayashi (1970), Lindzen (1974), Davies (1979), and many others developed a theory of large-scale tropical waves based on the hypothesis that wave-induced lifting rather than Ekman pumping forces convection. Convective heating in turn forces the wave. This theory became generally known as wave-CISK (wave-conditional instability of the second kind; Lindzen, 1974). Wave-CISK models tend to produce instabilities which have maximum growth rates at the shortest wavelengths.

Ooyama (1982) concluded that wave-CISK is nothing more than an aliased form of ordinary convective instability. Nevertheless, it tends to predict wave speeds which are commensurate with the observed speeds of tropical, convectively coupled Kelvin waves (Wheeler and Kiladis, 1999). The moisture convergence theory of Kuo (1965, 1974) is generally considered to be related closely to wave-CISK.

1.3 CAPE forcing

Theories of convective forcing based on control by convective available potential energy (CAPE) were developed about the same time as wave-CISK. These include the convective adjustment theory of Manabe et al. (1965) and the convective quasi-equilibrium theory of Arakawa and Schubert (1974). In both of these theories convection is assumed to respond nearly instantly to a tendency in CAPE (or a closely related quantity) so as to return this variable to the equilibrium value specific to the theory.

Cumulus parameterizations based on these ideas were developed, though the complexity of these models generally precludes their use in simplified linear contexts. One exception is the linearized Arakawa-Schubert model of Stark (1976), who found that tropical wave modes tended to be neutral rather than unstable for realistic conditions. Another is the theory of Neelin and Yu (1994), which uses a simplified version of the Betts-Miller

(1986) convective adjustment scheme. This theory also produces only damped modes unless some independent destabilizing mechanism is introduced.

1.4 Strict quasi-equilibrium

Emanuel (1987) introduced a model of intraseasonal oscillations based on the simple idea of strict quasi-equilibrium. In this theory convection is assumed to drive the atmosphere instantly to a moist adiabat consistent with the equivalent potential temperature of the boundary layer. The latter is determined by the interaction of surface fluxes, radiation, and vertical motion. In a mean easterly flow, the enhancement of surface fluxes associated with stronger than normal easterlies results in the development of unstable eastward-propagating large-scale waves by the so-called WISHE process (wind induced surface heat exchange). These waves are highly dispersive, with 30 m s^{-1} phase speeds for long wavelengths, decreasing significantly for shorter wavelengths.

Various elaborations of this theory have been proposed, e. g., Yano and Emanuel (1991), Emanuel (1993), Emanuel et al. (1994), Neelin and Yu (1994), but all retain the same general characteristics. In particular, the vertical wave structure in all of these cases is that of the first baroclinic mode, with a vertical half-wavelength equal to the depth of the troposphere. Phase speeds are reduced from free gravity wave values by virtue of an effective static stability in which condensational heating partially compensates cooling due to dry adiabatic lifting.

Given the rapid propagation speeds, it is hard to see how these modes can be related to intraseasonal oscillations such as the Madden-Julian oscillation (Madden and Julian, 1994). Various tests of the strict quasi-equilibrium hypothesis are not encouraging. Brown and Bretherton (1997) found that the increase in the mean temperature of the troposphere associated with an increase in the boundary layer equivalent potential temperature is only a third to a half of what might be expected from strict quasi-equilibrium. Even worse, the observed response of the atmosphere to intense convection is universally cooling in the lower troposphere and warming in the upper troposphere (Reed and Recker, 1971; Thompson et al. 1979; Cho and Jenkins, 1987; McBride and Frank, 1999). This change in thermal structure is related geostrophically to the development of mid-level cyclonic vorticity, which indicates that the convective tendency to produce a moist adiabat is not strong enough to overcome geostrophic adjustment.

Tropical wave disturbances have also been shown to have vertical profiles of temperature, heating, and vertical velocity which are more complex than hypothesized for strict quasi-equilibrium. Furthermore, this structure appears to be essential to the dynamics of these disturbances (Straub and Kiladis, 2002; Kiladis et al. 2005).

1.5 Two-component vertical structure

Recently a number of theories have attempted to take into account the observed vertical structure of tropical waves. Mapes (2000) developed a linearized model truncated at the first two vertical modes of Fulton and Schubert (1985). The first mode approximates the fundamental baroclinic mode of the tropical troposphere while the second (the stratiform

mode) has roughly half the vertical wavelength. Convective heating in the first mode is controlled by a combination of CAPE and the ratio of convective inhibition to boundary layer turbulent kinetic energy (CIN/K), while heating in the second mode is a lagged and scaled version of fundamental mode heating designed to approximate the effects of stratiform precipitation. When control by CIN/K is turned off, the model is stable and no wave disturbance develops. Such development only occurs when CIN/K is enabled, resulting in waves propagating at the speed of observed convectively coupled Kelvin waves.

Majda and Shefter (2001) and Majda et al. (2004) developed what appears to be a similar model, but without the dependence of convective heating on CIN/K. Curiously, these models produce instability even though they are forced only by CAPE.

1.6 Moisture mode

A variety of recent work has shown that tropical precipitation is very sensitive to the precipitable water in the troposphere (Sherwood, 1999; Lucas et al. 2000; Sobel et al. 2004; Bretherton et al. 2004; Derbyshire et al. 2004; Raymond and Zeng, 2005). Fuchs and Raymond (2002, 2005) developed a linear shallow water equation model in which precipitation is assumed to be proportional to precipitable water. WISHE and cloud-radiation interactions (CRI) are included. A single unstable mode develops in this model when either WISHE or CRI is turned on. Without WISHE (i. e., without surface heat flux variability resulting from zonal wind variability in the presence of mean easterlies), the mode is stationary; the effect of WISHE is to destabilize disturbances with small zonal wavenumber and make them propagate to the east. CRI results in instability insensitive to wavenumber. Since the precipitation in these modes depends on the existence of large moisture anomalies, we call them *moisture modes*.

Sobel and Horinouchi (2000) and Sobel et al. (2001) developed a theory of unstable, slowly propagating modes in an environment with a meridional moisture gradient which have the character of moisture modes. The gross moist stability (GMS; Neelin and Held, 1987) is assumed to be positive in their theory. When the GMS is greater than zero, instability vanishes for zero moisture gradient. However, examination of the theory reveals that instability persists in this case if the GMS is allowed to be negative.

Sobel and Bretherton (2003) showed that damped moisture modes exist in numerical model simulations of a homogeneous, non-rotating environment with parameterized convection. However, Grabowski (2003) found that the interaction of moisture fluctuations with deep convection was essential to the simulated development of the large-scale structure of tropical disturbances in a calculation in which convection was parameterized with a cumulus ensemble model in each grid box.

Given the apparent role of negative GMS in destabilizing moisture modes, we need to determine whether negative GMS actually occurs in the tropical environment. The observational results of López Carrillo and Raymond (2005) suggest that negative GMS occurs commonly over the west Pacific warm pool during relatively dry conditions in which convective systems exhibit little stratiform precipitation development, whereas positive GMS develops in moist situations with widespread deep convection and large stratiform rain areas.

1.7 Present work

The present paper continues our quest to find the minimal set of assumptions needed to explain the observed spectrum of tropical oceanic convection. It builds on the work of Fuchs and Raymond (2002) by expanding the shallow water dynamics of this model to full vertical resolution while retaining its cloud and precipitation physics. The primary goal is to clarify how the moisture instability of the earlier model presents itself in the vertically resolved case. In addition, we are able to cast some light on the dynamical nature of traveling convective modes such as the equatorial Kelvin mode, even though these modes do not amplify in the current context.

The model equations are described in section 2 and the dispersion relation for the disturbances is developed in section 3. Results are presented and discussed in section 4, and conclusions are drawn in section 5.

2 Model

We first present our linearized governing equations for large scale motions in a nonrotating atmosphere. Then we explain the thermodynamic forcing of the model, concentrating on its vertical structure.

2.1 Governing equations

Our two-dimensional, Boussinesq, linearized system of governing equations includes the horizontal momentum equation

$$\frac{\partial u}{\partial t} + \frac{\partial \Pi}{\partial x} = 0 \tag{1}$$

where u is the horizontal wind and Π is the mean potential temperature times the Exner function perturbation; the hydrostatic equation

$$\frac{\partial \Pi}{\partial z} - b = 0 \tag{2}$$

where b is the buoyancy perturbation (defined below); the continuity equation

$$\frac{\partial u}{\partial x} + \frac{\partial w}{\partial z} = 0 \tag{3}$$

with w the vertical velocity; the buoyancy equation

$$\frac{\partial b}{\partial t} + \Gamma_B w = S_B \tag{4}$$

with $\Gamma_B = (g/C_p)ds_{d0}/dz$ and $S_B = (g/C_p)ds_d/dt$, where g equals the acceleration of gravity, C_p is the specific heat of air at constant pressure, and where the dry entropy is split into mean and perturbation parts $s_d = s_{d0}(z) + s'_d$ with $b = gs'_d/C_p$; the moisture equation

$$\frac{\partial q}{\partial t} + \Gamma_Q w = S_Q \tag{5}$$

with $\Gamma_Q = (gL/C_pT_R)dr_0/dz$ and $S_Q = (gL/C_pT_R)dr/dt$ where the mixing ratio $r = r_0(z) + r'$, L is the latent heat of condensation, $T_R = 300$ K is a constant reference temperature, and $q = (gL/C_pT_R)r'$; and finally the moist entropy equation

$$\frac{\partial e}{\partial t} + \Gamma_E w = S_E \tag{6}$$

with $\Gamma_E = (g/C_p)ds_0/dz$ and $S_E = (g/C_p)ds/dt$, where the moist entropy $s = s_0(z) + s'$ and $e = (g/C_p)s'$.

The last three equations are not independent. Note that $e = b + q$ and $\Gamma_E = \Gamma_B + \Gamma_Q$. We assume that Γ_B is constant. The vertical structure of Γ_E is discussed later.

2.2 Thermal assumptions of the model

As in Fuchs and Raymond (2002, 2005) we assume that the vertically integrated dry entropy source term S_B depends on the precipitation rate minus the radiative cooling rate, the integrated moisture source term S_Q depends on evaporation rate minus the precipitation rate, and the integrated moist entropy source term S_E on evaporation rate minus the radiative cooling rate,

$$B = \int_0^h S_B(z)dz = P - R \tag{7}$$

$$Q = \int_0^h S_Q(z)dz = E - P \tag{8}$$

$$\Xi = \int_0^h S_E(z)dz = E - R \tag{9}$$

where h is the depth of the troposphere and P, E, and R are scaled perturbations in the precipitation rate, the surface evaporation rate, and the vertically integrated radiative cooling rate. Note that $\Xi = B + Q$.

The fundamental assumptions of the model are that the perturbation precipitation rate is proportional to the perturbation precipitable water

$$P = \alpha \int_0^h q(z)dz \tag{10}$$

where $\alpha = 1$ d^{-1} is moisture relaxation rate; that the perturbation radiative cooling rate decreases as the perturbation precipitation rate increases due to the blocking of outgoing longwave radiation by the associated clouds

$$R = -\alpha\varepsilon \int_0^h q(z)dz \tag{11}$$

where ε is the cloud-radiative feedback parameter taken as $\varepsilon \approx 0.2$ (see Fuchs and Raymond, 2002); and where the surface perturbation evaporation rate is given by

$$E = \frac{C\Delta q U u_s}{(U^2 + W^2)^{1/2}} \tag{12}$$

where C is the transfer coefficient, Δq is the scaled difference between the saturation mixing ratio at the sea surface temperature and the subcloud mixing ratio, U is the ambient zonal wind at the surface, $W \approx 3$ m s^{-1} is a constant needed to account for gustiness, and u_s is the perturbation surface zonal wind. For strong ambient easterly winds in this linearized parameterization of WISHE, $U/(U^2 + W^2)^{1/2} \approx -1$. The surface sensible heat fluxes are ignored as they are small compared to the latent heat fluxes over the tropical oceans.

Equations (7) - (12) are general in the sense that no assumptions have been made yet about the vertical structure of the fields. At this point Fuchs and Raymond (2002, 2005) imposed a first baroclinic mode vertical structure on all variables. We believe that the first baroclinic mode approximation is the weakest part of the previous model. In this paper we calculate the vertical profiles of all the variables on the assumption that only the vertical heating profile is fixed. We thus exclude the separate vertical heating profiles for cumulus congestus, deep convection, and stratiform conditions assumed by Mapes (2000), Majda and Shefter (2001), and Majda et al. (2004).

2.3 Vertical velocity

We assume that all the variables are proportional to $\exp[i(kx - \omega t)]$ where k is the zonal wavenumber and ω is the frequency. From the governing system of equations (1) - (4), we derive the inhomogeneous differential equation for vertical velocity perturbation:

$$\frac{d^2 w(z)}{dz^2} + m^2 w(z) = \frac{k^2}{\omega^2} S_B(z) \tag{13}$$

where $m = k\Gamma_B^{1/2}/\omega$. To solve (13) we assume that the heating has a fixed vertical profile: $S_B(z) = B\eta(z)$ where $\eta(z)$ is nonzero only in the troposphere $0 < z < h$ and where

$$\int_0^h \eta(z) dz = 1 \tag{14}$$

We do not need to know the vertical profiles of $S_Q(z)$ and $S_E(z)$.

From Raymond (1975)

$$w(z) = [I_2(z) - I_1(0)]\, w_{1H}(z) + I_1(z) w_{2H}(z) \tag{15}$$

where the homogeneous solutions to (13) are $w_{1H} = \exp(-imz)$ and $w_{2H} = \exp(imz)$ and where $I_1(z)$ and $I_2(z)$ are given by:

$$I_1(z) = \frac{ik^2}{2m\omega^2} B \int_z^h w_{1H}(z')\eta(z') dz' \tag{16}$$

$$I_2(z) = \frac{ik^2}{2m\omega^2} B \int_0^z w_{2H}(z')\eta(z')dz' \tag{17}$$

This solution has $w = 0$ at the surface and upward radiation boundary conditions built into it.

We assume here a simple heating profile that satisfies (14) $\eta(z) = (m_0/2)\sin(m_0 z)$ for $z \leq h$, where $m_0 = \pi/h$. The resulting vertical velocity profile in the troposphere is

$$w(z) = \frac{m_0 B}{2\Gamma_B(1-\Phi^2)} \left[\sin(m_0 z) + \Phi \exp(-i\pi/\Phi)\sin(mz)\right] \qquad z \leq h, \tag{18}$$

where

$$\Phi = \frac{m_0}{m} = \frac{\pi}{mh} = \frac{\pi\omega}{hk\Gamma_B^{1/2}} = \frac{\Omega}{\kappa} \tag{19}$$

is the dimensionless phase speed. We scale the frequency with the moisture relaxation constant α so that $\Omega = \omega/\alpha$ is the dimensionless frequency. Similarly we define a dimensionless wavenumber $\kappa = h\Gamma_B^{1/2}k/(\pi\alpha)$. Velocities scale with the phase speed of free gravity waves with fundamental baroclinic mode vertical structure, $h\Gamma_B^{1/2}/\pi$. The inhomogeneous solution $\sin(m_0 z)$ in (18) is driven by the deep convective heating component while the homogeneous solution $\exp(-i\pi/\Phi)\sin(mz)$ represents the free gravity wave which is needed to satisfy the radiation boundary condition at $z = h$. The vertical velocity perturbation in the stratosphere is:

$$w(z) = \frac{m_0 B\Phi}{2\Gamma_B(1-\Phi^2)} \sin(\pi/\Phi)\exp(-imz) \qquad z > h \tag{20}$$

3 Calculating the dispersion relation

The polarization relations for our system of equations are

$$u(z) = \frac{i}{k}\frac{\partial w(z)}{\partial z} \tag{21}$$

$$\Pi(z) = \frac{i\omega}{k^2}\frac{\partial w(z)}{\partial z} \tag{22}$$

$$b(z) = \frac{i}{\omega}\left(S_B(z) - \Gamma_B w(z)\right) \tag{23}$$

$$q(z) = \frac{i}{\omega}\left(S_Q(z) - \Gamma_Q(z) w(z)\right) \tag{24}$$

$$e(z) = \frac{i}{\omega}\left(S_E(z) - \Gamma_E(z) w(z)\right) \tag{25}$$

We now calculate the dispersion relation. Combining (7), (10), and (11), we find that

$$B = \int_0^h S_B(z)dz = P - R = \alpha(1+\varepsilon)\int_0^h q(z)dz \tag{26}$$

Recalling that $e = b + q$ we can further write:

$$B = \alpha(1+\varepsilon)\left(\int_0^h e(z)dz - \int_0^h b(z)dz\right) \tag{27}$$

It is straightforward to calculate the vertical integral of the scaled entropy perturbation b from the polarization relation (23):

$$\int_0^h b(z)dz = \frac{i}{\omega}\left[\int_0^h S_B(z)dz - \Gamma_B\int_0^h w(z)dz\right] \tag{28}$$

From (18) we find that

$$\int_0^h \Gamma_B w(z)dz = \frac{BF(\Phi)}{1-\Phi^2} \tag{29}$$

where

$$F(\Phi) = 1 + \frac{\Phi^2}{2}\exp\left(-i\frac{\pi}{\Phi}\right)\left[1 - \cos\left(\frac{\pi}{\Phi}\right)\right]. \tag{30}$$

The vertical integral of the moist entropy perturbation is obtained from (6):

$$-i\omega\int_0^h e(z)dz + \int \Gamma_E(z)w(z)dz = E - R \tag{31}$$

Recalling the expressions (11) and (12) for radiative cooling rate and the surface evaporation rate we get

$$\int_0^h e(z)dz = \frac{1}{\alpha\varepsilon + i\omega}\left[\int_0^h \Gamma_E(z)w(z)dz + \alpha\varepsilon\int_0^h b(z)dz - CUu_s\Delta q/(U^2+W^2)^{1/2}\right] \tag{32}$$

We are now ready to write the equation for B from which the dispersion relation is calculated. We substitute (32) and (28) into (27), arriving at

$$(i\kappa\Phi - 1)B = (1+\varepsilon)\left(\int_0^h \Gamma_E(z)w(z)dz - \int_0^h \Gamma_B w(z)dz - CUu_s\Delta q/(U^2+W^2)^{1/2}\right) \tag{33}$$

From (21) we find that

$$u_s = \frac{i}{\kappa}\left(\frac{\partial w}{\partial z}\right)_{z=0} = i\frac{m_0^2 BG(\Phi)}{2k\Gamma_B(1-\Phi^2)} \tag{34}$$

where

$$G(\Phi) = 1 + \exp(-i\pi/\Phi), \tag{35}$$

which allows us to compute the WISHE term $CUu_s\Delta q/(U^2+W^2)^{1/2}$.

3.1 The gross moist stability

The first term on the right side of (32) requires some additional assumptions about the form of the ambient moist entropy profile. We write a nondimensionalized gross moist stability (GMS) Γ_M as

$$\Gamma_M = \frac{\int_0^h \Gamma_E(z) w(z) dz}{\int_0^h \Gamma_B w(z) dz} \tag{36}$$

where the denominator is given by (29) and where

$$\Gamma_E(z) = \frac{g}{C_p} \frac{ds_0(z)}{dz} \equiv \frac{de_0(z)}{dz}. \tag{37}$$

The quantity s_0 is the mean moist entropy profile and e_0 is the scaled moist entropy profile. (This differs somewhat from Neelin and Held's (1987) GMS; integrating the numerator by parts. replacing the denominator by the mass flow through the system, and assuming $w = 0$ at the tropopause yields something closer to their original definition. The use of moist entropy rather than moist static energy as the thermodynamic variable constitutes an insignificant difference in this case.)

To estimate the value of Γ_M in our model we assume that the scaled mean moist entropy e_0 has the form shown in figure 1. We also assume that the moist entropy takes the same value at the top of the troposphere as at the surface. We can then write the moist static stability

$$\Gamma_E = \begin{cases} -\triangle e_0/d, & 0 < z < d \\ \triangle e_0/(h-d), & d < z < h \end{cases} . \tag{38}$$

The integral in the numerator of (36) is

$$\int_0^h \Gamma_E(z) w(z) dz = \frac{B \Delta e J(H, \Phi)}{2(1-\Phi^2) H (1-H)} \tag{39}$$

where $\Delta e = \Delta e_0 / h \Gamma_B$ is the nondimensionalized scaled moist entropy difference,

$$J(H,\Phi) = 2H - 1 + \cos(\pi H) + \Phi^2 \exp\left(-i\frac{\pi}{\Phi}\right)\left[H - 1 - H\cos\left(\frac{\pi}{\Phi}\right) + \cos\left(\frac{\pi H}{\Phi}\right)\right], \tag{40}$$

and where $H = d/h$ is the nondimensionalized height of minimum entropy.

In this formulation the GMS is a function of Φ:

$$\Gamma_M = \frac{\Delta e J(H,\Phi)}{2H(1-H)F(\Phi)} \tag{41}$$

where $F(\Phi)$ is defined in (30). However, in the limit in which $|\Phi|^2 \ll 1$, the GMS takes the approximate form

$$\Gamma_M \approx \frac{\Delta e[2H - 1 + \cos(\pi H)]}{2H(1-H)}. \tag{42}$$

3.2 Dispersion relation

We now substitute (29), (39), and (34) into (33) and use the definition of GMS (36) to write the dispersion relation:

$$\kappa\Phi^3 + i\Phi^2 - \kappa\Phi - i + i(1+\varepsilon)(1-\Gamma_M)F(\Phi) - \frac{\Lambda}{\kappa}G(\Phi) = 0 \tag{43}$$

where $F(\Phi)$ is defined by (30), $G(\Phi)$ by (35), and where $\Lambda = m_0 CU\Delta q(1+\varepsilon)/[2\alpha\Gamma_B^{1/2}(U^2+W^2)^{1/2}]$ is the WISHE parameter. The parameters we vary are Δe, H, ε, and Λ.

4 Results and discussion

Figure 2 shows phase speeds and growth rates plotted against planetary wavenumber l (wavelength divided by the circumference of the earth, assumed to be 40000 km) for all modes predicted by the dispersion relation (43). These include convectively coupled gravity modes, fast gravity modes, and the moisture mode. In this control case CRI and WISHE are turned on with $\varepsilon = 0.2$ and $\Lambda = -0.4$. The entropy profile parameters take the values $H = 0.5$ and $\Delta e = 0.26$, which corresponds to a mean moist entropy difference $\Delta s_0 = 40$ J kg^{-1} K^{-1} and a minimum in ambient moist entropy at half the height of the tropopause. In this case the GMS $\Gamma_M \approx 0$.

In order better to understand these modes, we investigate the vertical velocity and buoyancy perturbations for neutral modes in an environment with a rigid lid. These variables take particularly simple forms in this case, and insight garnered with these solutions helps us understand the more complex case with growing or decaying modes and an upward radiation boundary condition.

Assuming as before that $S_B = (m_0 B/2)\sin(m_0 z)$ where $m_0 = \pi/h$ with h being the depth of the troposphere, the general solution to (13) satisfying rigid lid boundary conditions at $z = 0$, h is

$$w = \frac{m_0 B}{2\Gamma_B(1-\Phi^2)}\sin(m_0 z) + A\sin(mz) \tag{44}$$

where $m = m_0/\Phi$, A is an arbitrary constant multiplying the homogeneous part of the solution to (13), and where the dimensionless phase speed of the mode is $\Phi = 1/n$ for $n = 2, 3, 4, \ldots$. The constraint on Φ^{-1} to integer values comes from the upper rigid lid condition. We have omitted consideration of the possibility that $\Phi = 1$, which explains the absence of $n = 1$, since an alternate treatment of the inhomogeneous part of the solution is required in this case. The corresponding solution for the buoyancy perturbation (23) is

$$b = \frac{1}{i\omega}\left(\frac{m_0 B\Phi^2}{2(1-\Phi^2)}\sin(m_0 z) - \Gamma_B A\sin(m_0 z/\Phi)\right). \tag{45}$$

An alternate possibility is that $A = 0$, i. e., the homogeneous part of the solution vanishes. In this case there is no requirement that the dimensionless propagation speed be quantized by the rigid lid condition – it can take on arbitrary values, excluding $\Phi = 1$.

4.1 Convectively coupled gravity modes

The convectively coupled gravity modes move with phase speeds ranging from 19 m s^{-1} for long wavelengths to 16.5 m s^{-1} for short wavelengths in the control simulation of figure 2. As figure 3 shows, the characteristics of these modes are relatively insensitive to changes in the vertical profile of moist entropy. In all cases the phase speed is only a weak function of wavenumber, indicating that the modes are only modestly dispersive.

As figure 4 shows, the buoyancy anomaly in this mode is positively correlated with the heating in the mid-troposphere where the heating is the strongest, which means that available potential energy is being added to the wave. In spite of this, the wave is damped, as indicated by the increasing amplitude with height. It also does not have the characteristic "boomerang" structure in the vertical seen by Wheeler et al. (2000) and Straub and Kiladis (2002). In spite of this, the wave is interesting because it moves at the observed speed of convectively coupled equatorial Kelvin waves and it has the potential to be destabilized by various mechanisms not included in the current model.

The propagation speed of this mode is similar to that seen in Mapes (2000), Majda and Shefter (2001), Majda et al. (2004), as well as in a host of wave-CISK models. We believe that this is not a coincidence, but results from the quantization of the vertical wavelength of the homogeneous part of the vertical velocity. The presence of a homogeneous part with $n \geq 2$ and significant magnitude is required for the buoyancy anomaly to change sign with height. This sign change is necessary for the wave-CISK mechanism to work; the low-level lifting which triggers convection in wave-CISK is associated with a negative buoyancy anomaly at low levels. However, a positive buoyancy anomaly colocated with the convection is needed at upper levels to allow the production of the available potential energy need for the disturbance to intensify. Similar considerations apply to the mechanisms in the rest of the above-mentioned models.

When the upper rigid lid is replaced by an upper radiation condition, the quantization of the vertical wavelength still occurs, but the actual quantized values are not as simply calculated. However, in general they do not differ radically from the values obtained in the rigid lid case. Thus the phase speeds computed in the two cases should be similar. The waves computed by Mapes (2000) and Majda and Shefter (2001) impose a quantization value of $n = 2$ by hypothesis, i. e., the homogeneous mode is a first harmonic. Our results for the (damped) convectively coupled gravity mode correspond more closely to a value of $n = 3$ (see figure 5), as is suggested in observations of equatorial waves by Wheeler et al. (2000) and Straub and Kiladis (2002).

Strict quasi-equilibrium disturbances exhibit a very different mechanism governing propagation. By hypothesis, the buoyancy anomaly in strict quasi-equilibrium does not change sign with height. Furthermore, these modes tend to be highly dispersive (e. g., Emanuel, 1987 and subsequent papers; Neelin and Yu, 1994), suggesting that their phase speeds are not constrained by the quantization of vertical wavelength discussed above. This is consistent with the absence of a homogeneous component in their solutions. The eastward propagation of these modes is actually due to a phase lag between heating and temperature which is related to the east-west asymmetry in surface fluxes in the presence of a mean easterly flow.

4.2 Fast gravity modes

The modeled fast gravity modes are only weakly coupled to convection. They have a phase speed near 48 m s^{-1} and decay at a very slow rate. Their vertical wavelength is approximately twice the depth of the troposphere, so they have a first baroclinic mode structure in the vertical. As these modes are of limited meteorological interest, we will not discuss them further here.

4.3 Moisture mode

The moisture mode shown on figure 2 is unstable and has properties nearly identical to the mode described by Fuchs and Raymond (2002, 2005). Since normally $\varepsilon \ll 1$ and $\Gamma_M \ll 1$, this mode has $|\Phi|^2 \ll 1$. The dispersion relation (43) reduces approximately to

$$\Phi = i(\varepsilon - \Gamma_M)/\kappa - \Lambda/\kappa^2. \tag{46}$$

under these conditions. This turns out to be consistent with the results obtained using the weak temperature gradient approximation (WTG) of Sobel et al. (2001) in the limit of zero meridional moisture gradient. In the context of our model, WTG is equivalent to setting the buoyancy perturbation $b = 0$ in the governing equations (1) - (6).

As (46) shows, the moisture mode is unstable when an "effective GMS" equal to $\Gamma_M - \varepsilon < 0$. The only effect of WISHE is to cause the disturbance to propagate, with the long wavelength modes propagating most rapidly. The direction of propagation is opposite the direction of the low-level zonal wind. The results for the moisture mode shown in figure 2 are consistent with (46), so this approximate dispersion relation is in good agreement with the full dispersion relation (43) in the case of the moisture mode. As expected, the approximate dispersion relation eliminates all gravity modes.

In contrast to the gravity modes, the homogeneous part of the solution to (13) plays only a minor role in the profile of vertical velocity for the moisture mode (see figure 6). The vertical velocity thus is proportional to the heating profile to a high degree of accuracy. The heating and temperature structure shown in figure 7 are also consistent with a fundamental baroclinic vertical mode structure.

The instability of the moisture mode depends on the existence of negative effective GMS. Neelin and Held (1987) and Sobel et al. (2001) (who did not include the effects of cloud-radiation interactions) assumed that the GMS Γ_M is always positive. However, López and Raymond (2005) found that negative GMS is associated with periods of widely scattered convection lacking significant stratiform rain, whereas positive GMS occurs when stratiform rain is widespread.

We speculate that the red noise part of the frequency-zonal wavenumber spectrum eliminated by Wheeler and Kiladis (1999) from their observational analysis of equatorial waves is actually a manifestation of moisture instability. One can imagine a life cycle of a disturbance which starts with showery convection manifesting negative GMS, proceeds to heavier rain accompanied by increasing stratiform conditions, and dies as the GMS turns positive and the instability vanishes. Given the lack of wavenumber selectivity in the disturbance growth rate, we envision an ensemble of nearly stationary disturbances of

widely varying sizes going through their life cycles with the chaotic behavior of a boiling pot of water. Most of the convection over the warm ocean regions of the tropics exhibits such behavior, and much of the equatorial precipitation may therefore be associated with such moisture modes.

5 Conclusions

This paper extends the shallow water model of Fuchs and Raymond (2002) to the vertically resolved case without changing the assumptions about precipitation production. The results are as follows:

1. The moisture mode found in the vertically resolved model has very similar characteristics to that seen in the earlier model. However, the vertically resolved calculation clarifies the role of gross moist stability in the production of instability. In particular, the moisture mode is unstable when a modified gross moist instability which includes the effects of cloud-radiation interactions is negative. We speculate that much of the non-wave deep convection in the equatorial regions is associated with unstable moisture mode disturbances. The moisture mode is retained when the dynamics are simplified to the weak temperature gradient approximation of Sobel et al. (2001).

2. The fast gravity modes seen by Fuchs and Raymond (2002) are seen in the present analysis as well. These modes have a fundamental baroclinic mode vertical structure, move with phase speeds of order 50 m s^{-1}, and interact only weakly with deep convection.

3. A more slowly propagating, convectively coupled gravity mode not found by Fuchs and Raymond (2002) is seen in the present results. This mode decays with time and propagates with a speed of $16 - 19$ m s^{-1}. The vertical structure is complex, consisting of an inhomogeneous part (in a mathematical sense) with a vertical velocity profile proportional to the convective heating profile, and a homogeneous part with a shorter wavelength governed by the upper radiation boundary condition. This wavelength determines the propagation speed of the mode. It is tempting to identify this mode with equatorial, convectively coupled Kelvin waves. However, additional precipitation physics beyond that used in the present model is presumably needed to give this mode its observed unstable behavior. Further progress in understanding equatorial Kelvin waves depends on elucidating the additional precipitation physics.

4. The amplitude of the homogeneous part of the solution in the convectively coupled gravity mode depends on the nature of the convective parameterization used in the model. Those which depend strongly on having a temperature perturbation which changes sign with height such as wave-CISK, the model of Mapes (2000), and the present model, need this homogeneous component. Its vertical wavelength in turn fixes the propagation speed of the disturbance. Strict quasi-equilibrium prohibits

such a temperature structure by hypothesis, and is therefore not subject to the constraint on the propagation speed imposed by the homogenous component of the solution. As a result, strict quasi-equilibrium models, especially those dependent on WISHE to induce propagation, can produce highly dispersive modes in which the propagation speed depends strongly on zonal wavenumber. The moisture mode has this characteristic in contrast to the convectively coupled gravity mode.

Acknowledgments. We thank Adam Sobel and Roger Smith for their useful comments. This work was supported by National Science Foundation Grant ATM-0352639.

REFERENCES

Arakawa, A. and Schubert, W. H. 1974. Interaction of a cumulus cloud ensemble with the large-scale environment. Part I. *J. Atmos. Sci.,* **31,** 674-701.

Battisti, D. S., Sarachik, E. S. and Hirst, A. C. 1999. A consistent model for the large-scale steady surface atmospheric circulation in the tropics. *J. Climate,* **12,** 2956-2964.

Betts, A. K. and Miller, M. J. 1986. A new convective adjustment scheme. Part II: Single column tests using GATE wave, BOMEX, ATEX and arctic air-mass data sets. *Quart. J. Roy. Meteor. Soc.,* **112,** 693-709.

Bretherton, C. S., Peters, M. E. and Back, L. E. 2004. Relationships between water vapor path and precipitation over the tropical oceans. *J. Climate,* **17,** 1517-1528.

Brown, R. G. and Bretherton, C. S. 1997. A test of the strict quasi-equilibrium theory on long time and space scales. *J. Atmos. Sci.,* **54**, 624-638.

Charney, J. 1971. Tropical cyclogenesis and the formation of the intertropical convergence zone. *Lectures in Applied Mathematics. American Mathematical Society,* **13**, 355-368.

Charney, J. G. and Eliassen, A. 1964. On the growth of the hurricane depression. *J. Atmos. Sci.,* **21**, 68-75.

Cho, H.-R. and Jenkins, M. A. 1987. The thermal structure of tropical easterly waves. *J. Atmos. Sci.,* **44**, 2531-2539.

Davies, H. C. 1979. Phase-lagged wave-CISK. *Quart. J. Roy. Meteor. Soc.,* **105**, 325-353.

Derbyshire, S. H., Beau, I., Bechtold, P., Grandpeix, J.-Y., Piriou, J.-M., Redelsperger, J.-L. and Soares, P. M. M. 2004. Sensitivity of moist convection to environmental humidity. *Quart. J. Roy. Meteor. Soc.,* **130**, 3055-3079.

Emanuel, K. A. 1987. An air-sea interaction model of intraseasonal oscillations in the tropics. *J. Atmos. Sci.,* **44**, 2324-2340.

Emanuel, K. 1993. The effect of convective response time on WISHE modes. *J. Atmos. Sci.,* **50**, 1763-1775.

Emanuel, K. A., Neelin, J. D. and Bretherton, C. S. 1994. On large-scale circulations in convecting atmospheres. *Quart. J. Roy. Meteor. Soc.,* **120**, 1111-1143.

Fuchs, Ž. and Raymond, D. J. 2002. Large-scale modes of a nonrotating atmosphere with water vapor and cloud-radiation feedbacks. *J. Atmos. Sci.,* **59**, 1669-1679.

Fuchs, Ž. and Raymond, D. J. 2005. Large-scale modes in a rotating atmosphere with radiative-convective instability and WISHE. *J. Atmos. Sci.,* **62**, 4084-4094.

Fulton, S. R. and Schubert, W. H. 1985. Vertical normal mode transforms: Theory and application. *Mon. Wea. Rev.,* **113**, 647-658.

Grabowski, W. W. 2003. MJO-Like coherent structures: Sensitivity simulations using the cloud-resolving convection parameterization (CRCP). *J. Atmos. Sci.,* **60**, 847-864.

Hayashi, Y. 1970. A theory of large-scale equatorial waves generated by condensation heat and accelerating the zonal wind. *J. Meteor. Soc. Japan,* **48**, 140-160.

Kiladis, G. N., Straub, K. H. and Haertel, P. T. 2005. Zonal and vertical structure of the Madden-Julian oscillation. *J. Atmos. Sci.,* **62**, 2790-2809.

Kuo, H. L. 1965. On the formation and intensification of tropical cyclones through latent heat release by cumulus convection. *J. Atmos. Sci.,* **22**, 40-63.

Kuo, H. L. 1974. Further studies of the parameterization of the influence of cumulus convection on large-scale flow. *J. Atmos. Sci.,* **31**, 1232-1240.

Lindzen, R. S. 1974. Wave-CISK in the tropics. *J. Atmos. Sci.,* **31,** 156-179.

Lindzen, R. S. and Nigam, S. 1987. On the role of sea surface temperature gradients in forcing low-level winds and convergence in the tropics. *J. Atmos. Sci.,* **44**, 2418-2436.

López Carrillo, C. and Raymond, D. J. 2005. Moisture tendency equations in a tropical atmosphere. *J. Atmos. Sci.,* **62**, 1601-1613.

Lucas, C., Zipser, E. J. and Ferrier, B. S. 2000. Sensitivity of tropical west Pacific oceanic squall lines to tropospheric wind and moisture profiles. *J. Atmos. Sci.,* **57**, 2351-2373.

Madden, R. A. and Julian, P. R. 1994. Observations of the 40-50 day tropical oscillation — a review. *Mon. Wea. Rev.,* **122**, 814-837.

Majda, A. J., Khouider, B., Kiladis, G. N., Straub, K. H. and Shefter, M. G. 2004. A model for convectively coupled tropical waves: Nonlinearity, rotation, and comparison with observations. *J. Atmos. Sci.,* **61**, 2188-2205.

Majda, A. J. and Shefter, M. G. 2001. Models for stratiform instability and convectively coupled waves. *J. Atmos. Sci.,* **58**, 1567-1584.

Manabe, S., Smagorinsky, J. and Strickler, R. F. 1965. Simulated climatology of a general circulation model with a hydrologic cycle. *Mon. Wea. Rev.,* **93**, 769-798.

Mapes, B. E. 2000. Convective inhibition, subgrid-scale triggering energy, and stratiform instability in a toy tropical wave model. *J. Atmos. Sci.,* **57**, 1515-1535.

McBride, J. L. and Frank W. M. 1999. Relationships between stability and monsoon convection. *J. Atmos. Sci.,* **56**, 24-36.

McGauley, M., Zhang, C. and Bond, N. A. 2004. Large-scale characteristics of the atmospheric boundary layer in the eastern Pacific cold tongue-ITCZ region. *J. Climate,* **17**, 3907-3920.

Moskowitz, B. M. and Bretherton, C. S. 2000. An analysis of frictional feedback on a moist equatorial Kelvin mode. *J. Atmos. Sci.,* **57**, 2188-2206.

Neelin, J. D. and Held, I. M. 1987. Modeling tropical convergence based on the moist static energy budget. *Mon. Wea. Rev.,* **115**, 3-12.

Neelin, J. D. and Yu, J.-Y. 1994. Modes of tropical variability under convective adjustment and the Madden-Julian oscillation. Part I: Analytical theory. *J. Atmos. Sci.,* **51**, 1876-1894.

Ooyama, K. 1982. Conceptual evolution of the theory and modeling of the tropical cyclone. *J. Meteor. Soc. Japan,* **60**, 369-379.

Raymond, D. J. 1975. A model for predicting the movement of continuously propagating convective storms. *J. Atmos. Sci.,* **32**, 1308-1317.

Raymond, D. J., Bretherton, C. S. and Molinari, J. 2006. Dynamics of the intertropical convergence zone of the east Pacific. *J. Atmos. Sci.,* **63**, 582-597.

Reed, R. J. and Recker, E. E. 1971. Structure and properties of synoptic-scale wave disturbances in the equatorial western Pacific. *J. Atmos. Sci.,* **28**, 1117-1133.

Sherwood, S. C. 1999. Convective precursors and predictability in the tropical western Pacific. *Mon. Wea. Rev.,* **127**, 2977-2991.

Sobel, A. H., Nilsson, J. and Polvani, L. M. 2001. The weak temperature gradient approximation and balanced tropical moisture waves. *J. Atmos. Sci.,* **58**, 3650-3665.

Sobel, A. H., Yuter, S. E., Bretherton, C. S and Kiladis, G. N. 2004. Large-scale meteorology and deep convection during TRMM KWAJEX. *Mon. Wea. Rev.,* **132**, 422-444.

Sobel, A. H. and Bretherton, C. S. 2003. Large-scale waves interacting with deep convection. *Tellus,* **55a**, 45-60.

Sobel, A. H. and Horinouchi, T. 2000. On the dynamics of easterly waves, monsoon depressions, and tropical depression type disturbances. *J. Meteor. Soc. Japan,* **78**, 167-173.

Stark, T. E. 1976. Wave-CISK and cumulus parameterization. *J. Atmos. Sci.,* **33**, 2383-2391.

Straub, K. H. and Kiladis, G. N. 2002. Observations of a convectively coupled Kelvin wave in the eastern Pacific ITCZ. *J. Atmos. Sci.,* **59**, 30-53.

Thompson, R. M., Payne, S. W., Recker, E. E. and Reed, R. J. 1979. Structure and properties of synoptic-scale wave disturbances in the intertropical convergence zone of the eastern Atlantic. *J. Atmos. Sci.,* **36**, 53-72.

Tomas, R. A., Holton, J. R. and Webster, P. J. 1999. The influence of cross-equatorial pressure gradients on the location of near-equatorial convection. *Quart. J. Roy. Meteor. Soc.,* **125**, 1107-1127.

Wang, B. and Rui, H. 1990. Dynamics of the coupled moist Kelvin-Rossby wave on an equatorial beta plane. *J. Atmos. Sci.,* **47**, 397-413.

Wheeler, M., Kiladis, G. N. and Webster, P. J. 2000. Large-scale dynamical fields associated with convectively coupled equatorial waves. *J. Atmos. Sci.,* **57**, 613-640.

Wheeler, M. and Kiladis, G. N. 1999. Convectively coupled equatorial waves: Analysis of clouds and temperature in the wavenumber-frequency domain. *J. Atmos. Sci.,* **56**, 374-399.

Yano, J.-I. and Emanuel, K. 1991. An improved model of the equatorial troposphere and its coupling with the stratosphere. *J. Atmos. Sci.,* **48**, 377-389.

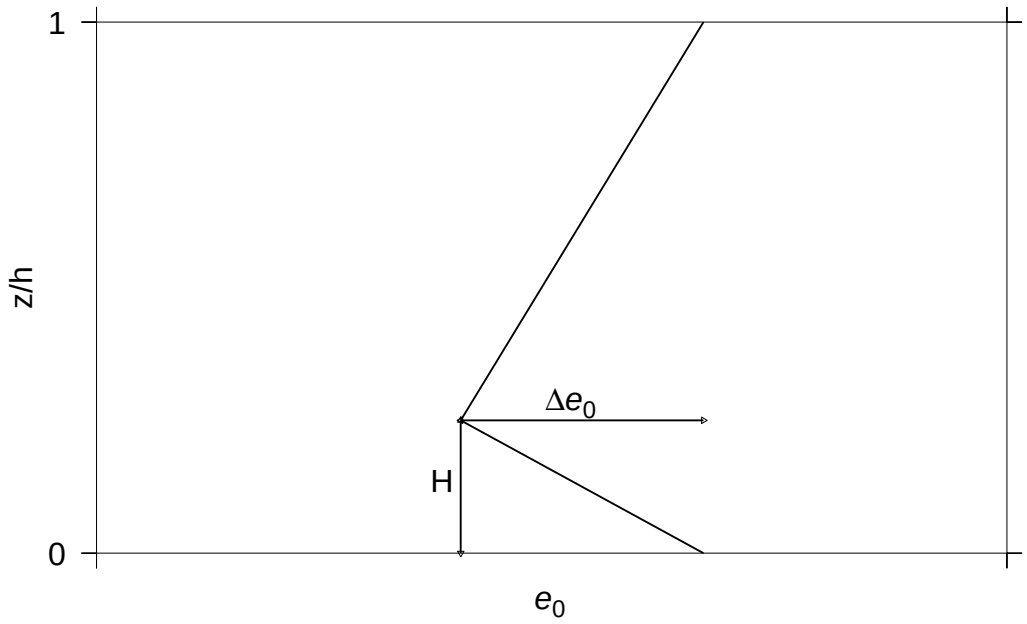

Figure 1: The scaled mean moist entropy profile as a function of nondimensionalized height.

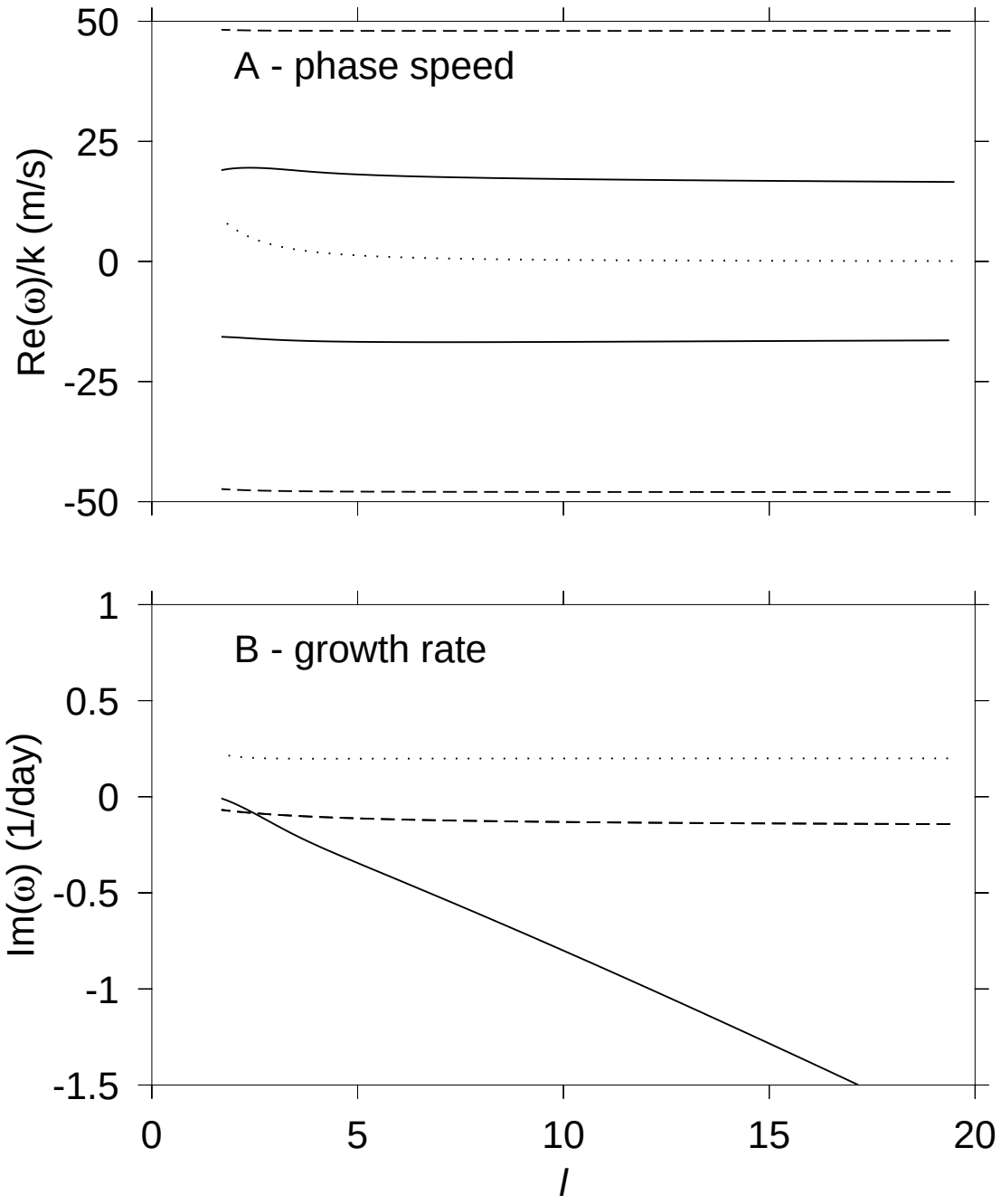

Figure 2: Dimensional dispersion curves as a function of the planetary wavenumber l when $\varepsilon = 0.2$, $\Lambda = -0.4$, $\Delta e = 0.26$, $H = 0.5$. Solid line represents convectively coupled gravity modes, dashed lines represent fast gravity modes and dotted line represents the moisture mode.

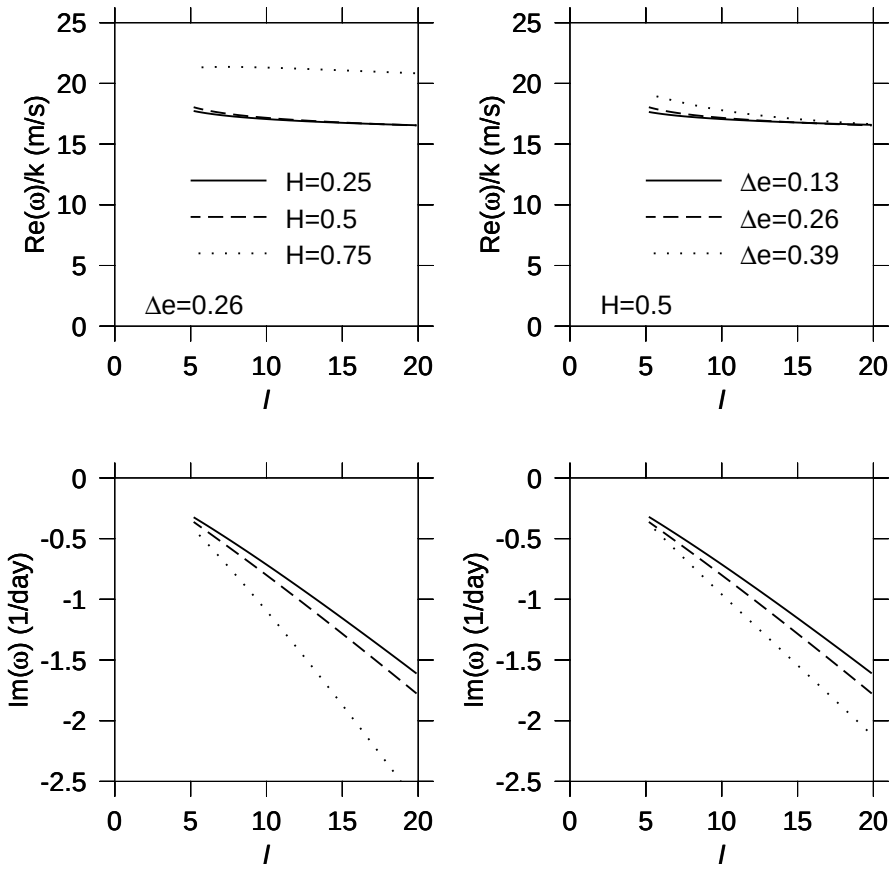

Figure 3: Dimensional dispersion curves of the convectively coupled gravity mode as a function of l for $\varepsilon = 0.2$, $\Lambda = -0.4$. The upper panels show the phase speed, the lower ones show the growth rate. On the left H is varied, while on the right we vary Δe.

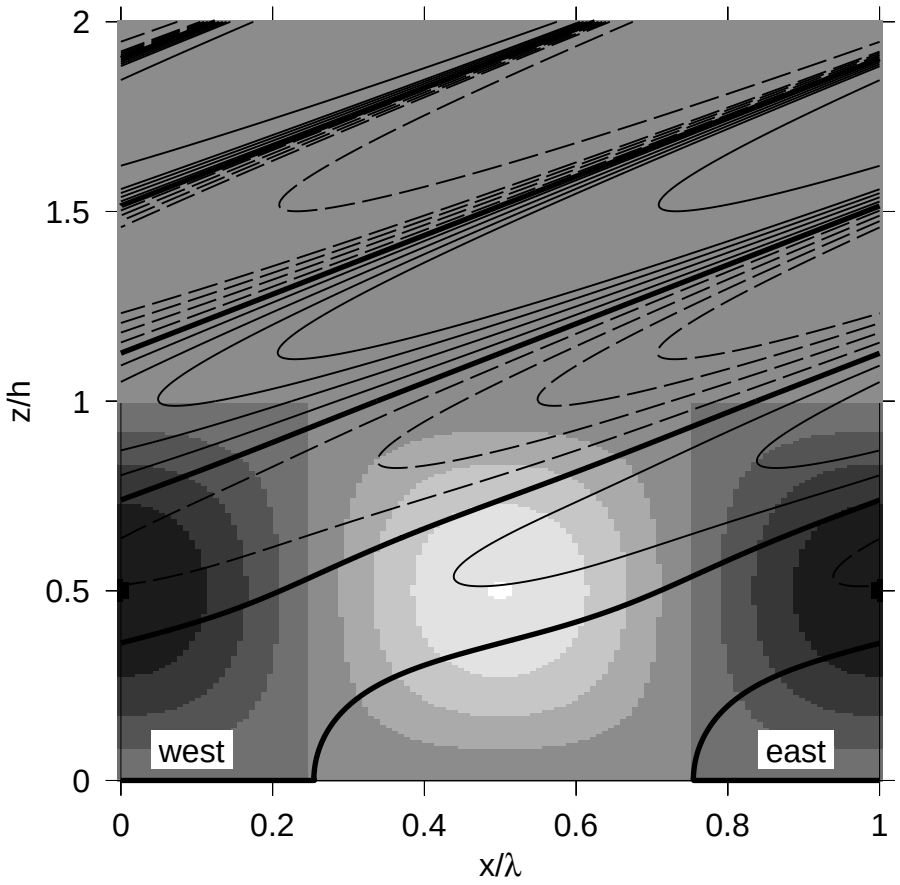

Figure 4: Heating and temperature for the convectively coupled gravity mode in the $z/h-x/\lambda$ plane for planetary wavenumber $l = 10$, where λ is the horizontal wavelength. The heating has maximum where the image is white and minimum for black. The buoyancy perturbation is given as a contour plot where the thick solid line corresponds to zero contour. Negative temperature perturbation contours are given as dashed line, while positive contours are solid. The contour interval is 0.5 in arbitrary units.

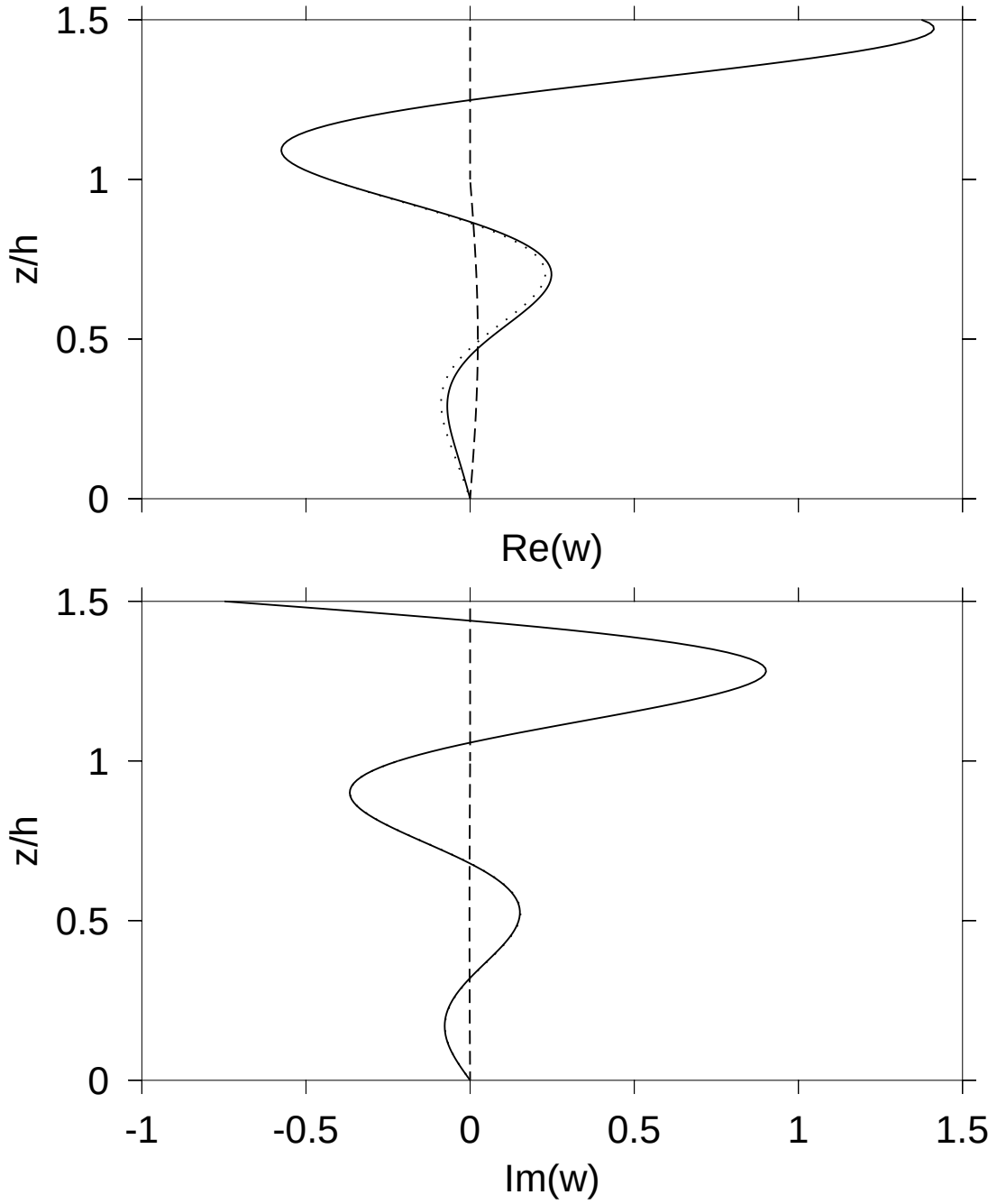

Figure 5: Vertical velocity perturbation as a function of height for the convectively coupled gravity mode with planetary wavenumber $l = 10$, $\Lambda = -0.4$, $\varepsilon = 0.2$, and $\Gamma_M \approx 0$. The upper panel represents the real part of vertical velocity and the lower panel the imaginary part. The solid line is for the total vertical velocity, the dashed line is for the inhomogeneous component of the solution, and the dotted line is for the homogeneous component.

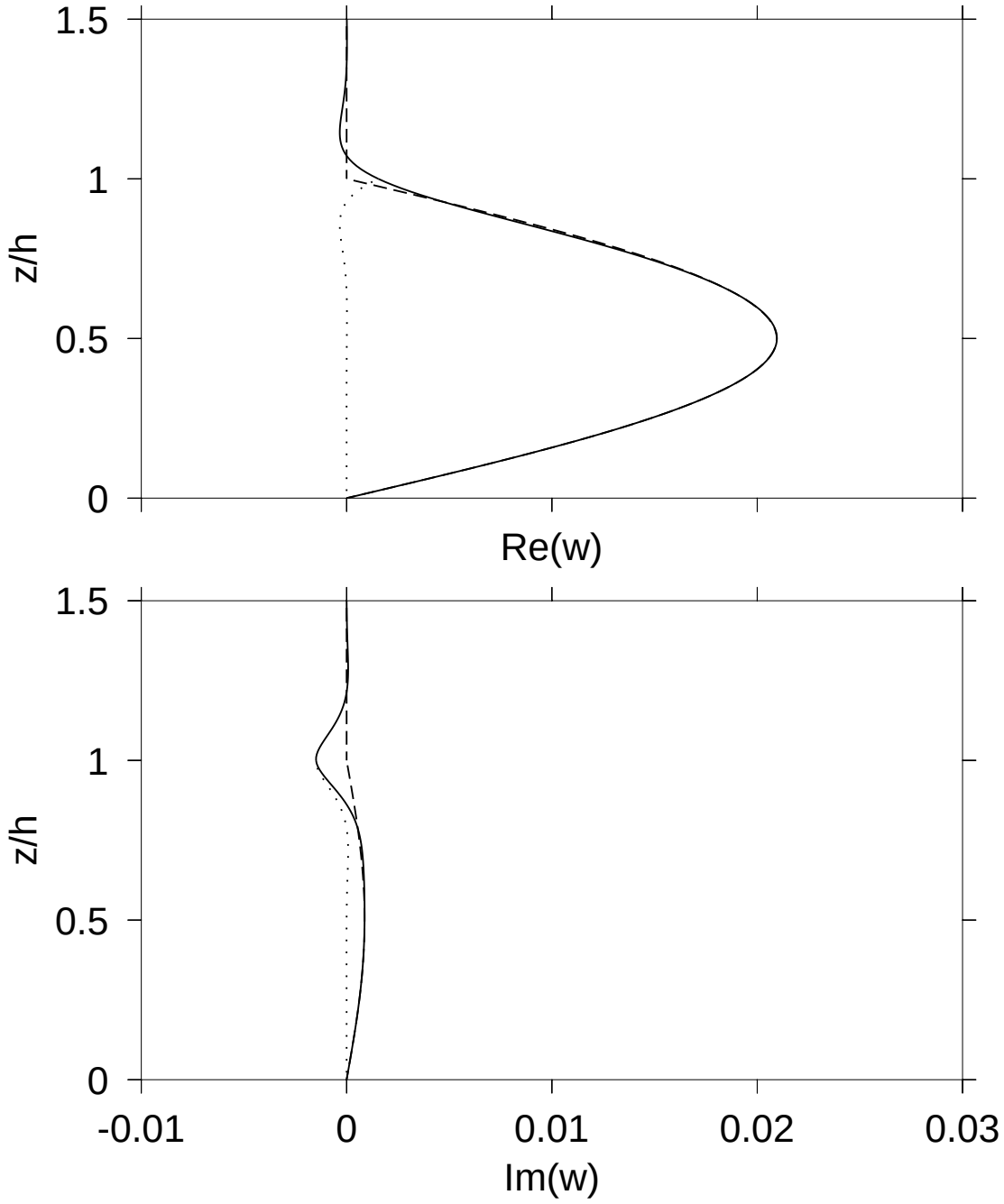

Figure 6: As in figure 5, but for the moisture mode with $l = 2$.

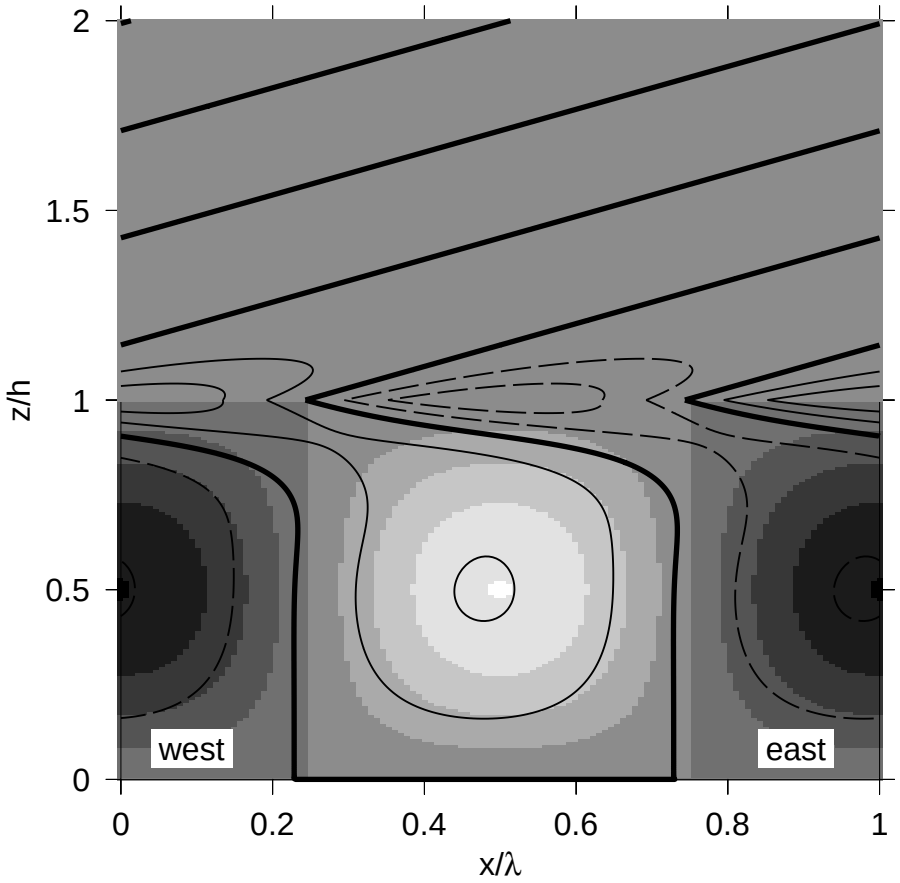

Figure 7: As in figure 4 except for the moisture mode with $l = 2$, $\Lambda = -0.4$, $\epsilon = 0.2$, and $\Gamma_M \approx 0$. The contour interval of temperature perturbation is 0.02 in arbitrary units, which is much finer than in figure 4.